

# RFI Localization in a Collaborative Navigation Environment

Naveed Ahmed, Nadezda Sokolova

*Department of Engineering Cybernetics, Norwegian University of Science and Technology, Trondheim, Norway*

## Abstract

Since the received GNSS signals are inherently very weak, a simple GNSS signal jammer can easily degrade the measurement quality, or completely deny GNSS signal reception at the receiver. In the context of collaborative navigation, the user-to-user radio links help the cooperating receivers/nodes to navigate in the compromised environment. Possibility to share information between the nodes allows not only for improving positioning and situational awareness of the cooperating group of users, but also for pro-active localization of the identified jamming source. The focus of this paper is on localization of Radio Frequency Interference (RFI) by a group of collaborating users. A synthetic array principle based on the Carrier-to-Noise Density Ratio ( $C/N_0$ ) measurements is used and applied to a multi-user scenario. To evaluate the performance of multi-user RFI localization, a series of experiments in a controlled lab environment have been carried out. This paper discusses the results as well as the limitations of the implemented technique.

## Keywords

RFI Localization, Carrier-to-Noise Density Ratio, Collaborative Navigation

## 1. Introduction

The signal strength of a GNSS signal, when it is received on the Earth, is merely -160 dBW (or 0.1fW) [1], which makes it vulnerable to signals that have higher power level and reside in the same frequency band. In some cases, it has also been reported that the signals that reside in the neighboring bands have some harmonics or the leakages that attempt to influence the GNSS signals. A large number of incidents involving GNSS interference observed by different GNSS-based service providers [2], as well as research projects aiming at mapping the frequency of RFI event occurrence [3] have shown how vulnerable the signals can be against ground-based emissions in and near the GNSS band, affecting and potentially disrupting its service.

To make a system resilient against GNSS signal jamming, we need to detect the source and mitigate its effects on the target receiver. Jamming source localization capability is also desirable in order to identify and prevent the disruption of system operations. Various techniques that range from the use of complex antenna designs for steering a null towards the angle of arrival of an undesired signal source from an airborne platform [4] to deploying complex ground-based infrastructure have been proposed. Jamming localization is typically performed by monitoring the GNSS signal bands and extracting certain parameters relating to e.g. the energy, angle, time, or frequency of the received source signal that can be used to determine position of the jammer.

---


*ICL-GNSS 2020 WiP Proceedings, June 02–04, 2020, Tampere, Finland*

✉ naveed.ahmed@ntnu.no (N. Ahmed); nadia.sokolova@itk.ntnu.no (N. Sokolova)

📞 0000-0002-4205-1733 (N. Ahmed)

© 2020 Copyright for this paper by its authors.

Use permitted under Creative Commons License Attribution 4.0 International (CC BY 4.0).

 CEUR Workshop Proceedings (CEUR-WS.org)

A broad overview of different available techniques for RFI localization is presented in [5]. The authors discuss the observables such as Received Signal Strength (RSS), Angle of Arrival (AOA), Time Difference of Arrival (TDOA), and Frequency Difference of Arrival (FDOA) or combination of these required for RFI source position estimation in a distributed network of nodes, and provide a comparative analysis of the techniques. RFI localization has also been demonstrated in [6] by studying the behavior of the Automatic Gain Control (AGC). In this work, a network of low-cost RF front ends is deployed in the vicinity of the RFI source and the AGC measurements are recorded and sent to a remote server to detect and localize the source. An antenna array based solution has been presented in [7] that exploits the RFI signal's Angle of Arrival (AOA) parameter to localize it. In this work, the system is tested with the WiFi signals without compromising the infrastructure in the vicinity of the receivers that is relying on the standard navigation systems. The jammer localization using Carrier-to-Noise density power ratio ( $C/N_0$ ) measurements has been demonstrated in [8], where authors present the solution to the localization problem for two cases. In the first case, a synthetic array based approach is used which suggests that a set of sensors in different positions in space can be replaced by a single sensor moving along a known trajectory taking measurements at different time instants. In the second case, a crowdsourcing approach is used and RFI detection and localization is performed using measurements simultaneously obtained from multiple static Android smartphones. Localization in this case is performed using the centroid approach.

Use of  $C/N_0$  measurements for jamming source localization is an attractive approach as it does not require any complex equipment and can be implemented using Commercial Off The Shelf (COTS) GNSS receivers. In this paper, we investigate the applicability of the synthetic array based technique presented in [8] by adopting the  $C/N_0$  measurements based RFI localization approach for a dynamic collaborating multi-user scenario.

The rest of the paper is organized as follows: Section 2 explains the RFI location technique for a single receiver case that is based on the synthetic array principle, section 3 provides a brief overview of the collaborative navigation along with certain considerations taken into account for this work, Section 4 discusses the localization technique for multi-user case, Section 5 briefly explains the experimental setup and scenario description, Section 6 presents and discusses the simulation results whereas, Section 7 draws the conclusion and points out the limitations and possible directions for the future work.

## 2. $C/N_0$ -based RFI Source Localization

A single receiver can localize the RFI source using the synthetic array principle that suggests that a set of sensors located at different positions can be replaced by a single sensor moving along a known trajectory [8]. Measurements recorded by the moving sensor are analogous to the output of elements or nodes of the physical antenna array. The synthetic array approach describes the variation of  $C/N_0$  as a function of the distance between the target receiver and interference source. An objective or cost function is defined by combining these  $C/N_0$  measurements obtained at various regular intervals. An extension of this approach for the multi-user case is explained later in Section IV. The jammer location is calculated by determining the global minima of the objective function. Following the approach presented in [8], a static jammer case is considered to explain the technique.

In the presence of a jamming signal, the effect of interference on signal quality is best

described by the effective  $C/N_0$  parameter [8], which can be expressed as

$$\left. \frac{C_i}{N_0} \right|_{eff} = \frac{C_i}{N_0} \left( \frac{1}{1 + k_\alpha \frac{J}{N_0}} \right) \quad (1)$$

where,  $C_i$  is the  $i^{th}$  satellite's received power,  $N_0$  is noise power spectral density,  $J$  is the received jamming signal power and  $k_\alpha$  is the Spectral Separation Coefficient, which is a factor that determines the degradation of actual  $C/N_0$  in presence of interference by determining the overlapping between power spectral densities of the received GNSS and interference signals[9]. Expressing the effective  $C/N_0$  model on a logarithmic scale and accounting for the jamming signal power path loss, the *effective*  $C/N_0$  can be reformulated as

$$\left. \frac{C_i}{N_0} \right|_{eff} = \beta_i + 10\alpha \log_{10}(d) \quad (2)$$

where  $\beta_i$  is obtained through receiver calibration,  $\alpha$  is the path loss exponent and  $d$  is the separation between the target receiver and the jammer. For some reference jammer power  $J_0$  observed at distance  $d_0$ ,  $\beta_i$  can be calculated using the following expression

$$\beta_i = \left. \frac{C_i}{N_0} \right|_{dB-Hz} - 10 \log_{10} \left( k_\alpha \frac{J_0}{N_0} \right) - 10\alpha \log_{10}(d_0) \quad (3)$$

As suggested in [8], the model defined in (2) stays valid for the average of effective  $C/N_0$  that is calculated for all the tracked satellites. The average effective  $C/N_0$  is mathematically given as

$$\frac{C_a}{N_0} = \frac{1}{N_{sat}} \sum_{i=0}^{N_{sat}-1} \frac{C_i}{N_0} \quad (4)$$

where,  $N_{sat}$  is the number of satellites the receiver is tracking. Using (4), model defined in (2) can be updated for all the available satellites and rewritten as

$$\left. \frac{C_a}{N_0} \right|_{eff} = \bar{\beta} + 10\alpha \log_{10}(d) \quad (5)$$

where,  $\bar{\beta}$  is same as  $\beta_i$  as explained above but this time  $\bar{\beta}$  is computed with respect to the average  $C/N_0$ . From processing point of view, measurements at various epochs are often desired and used in previously defined models. At any given instant  $n$ , (5) can now be written as

$$\left. \frac{C_a[n]}{N_0} \right|_{eff} = \bar{\beta} + 10\alpha \log_{10}(d[n]) \quad (6)$$

where, the distance  $d[n]$  between the jammer located at unknown location  $(x_j, y_j)$  and the receiver situated at  $(x[n], y[n])$  can be given as

$$d[n] = \sqrt{(x[n] - x_j)^2 + (y[n] - y_j)^2} \quad (7)$$

The objective function or cost function can now be formally defined as shown in (8) by substituting (7) in (6) and rearranging the resulting equation to bring all the parameters to

the right side of the equality sign. In this case, we attempt to employ the optimizer algorithm to calculate the point  $(x_j, y_j)$  at which global minima is achieved.

$$J(x_j, y_j) = \sum_{n=0}^{N-1} \left[ \frac{C_a[n]}{N_0} \Big|_{eff} - \bar{\beta} - 10\alpha \log_{10}(d[n]) \right]^2 \quad (8)$$

where,  $N$  is the number of instants for which the jamming event is observed and this factor reflects the size of synthetic array to be considered for localization purpose.  $N$  determines the length of synthetic array in terms of number of receiver position points. An expanded form of  $d[n]$  is not shown in (8) just for the sake of compactness but can be found in [8].

### 3. Collaborative Navigation System Overview

The notion of collaborative navigation system (CNS) is partially derived from the wireless sensor networks (WSNs). But unlike WSNs, the nodes in CNS aim to assist each other in navigating in the environment with reduced or compromised reception of GNSS signals. While a single, or multiple nodes within the network might experience reduced GNSS signal availability, collectively, the CNS may be able to receive enough GNSS signals augmented by inter-nodal ranging measurements and other navigation sensor data. The network is often designed to work in different configurations with node information processed either centrally or in a distributed manner. The generic key components of a node (building block of a CNS) include multiple sensors, signals and technologies, such as GNSS, WiFi, Inertial Measurement Units (IMUs), magnetometers, barometers, Visual Based Navigation (VBN) sensors, acoustic or Ultra Wide Band (UWB) signals, etc. [10][11]. Such design philosophy not only guarantees more accurate and reliable position solution but also provides better resilience against signal jamming.

To assist the nodes to navigate, the network functions by employing various information sharing mechanisms among the units or nodes. In a typical collaborative navigation scenario, the cooperating nodes exchanging range and other important information while having different levels of the reception of the GNSS signals. Within a network, the nodes could share the navigation states, uncertainty information, or the node to node range information (obtained using for example UWB radios). To maintain temporal situational awareness about the nodes' current states, they could store and forward the last detected or measured position along with its uncertainty. The detailed explanation of these mechanisms and their associated advantages and disadvantages are out the scope of this paper and could be found in [10],[11].

Due to the capability of the nodes to exchange information, positioning of all the nodes in the network can still be accomplished even if GNSS signal availability/quality at one or multiple nodes is degraded. And since to successfully disrupt the operation of the overall network, the majority of cooperating nodes must be compromised that is often difficult for a jamming source to accomplish, the cooperating systems are much harder to attack.

### 4. Collaborative RFI Source Localization

This section briefly explains the extension of the  $C/N_0$ -based RFI localization concept to incorporate the desired notion of collaboration. In the collaborative paradigm, all the cooperative nodes take part in the localization process. Since, each node is following its own trajectory, it would have its distinct impact on the overall solution. The core concept behind collaborative

RFI localization is same as that explained previously in section 2. Each of the cooperating nodes takes  $C/N_0$  measurements for all satellites in view at regular intervals and when the jamming signal is present determines the source location by solving for (8). By applying the synthetic array principle on each of the nodes, the capability of single node to determine jammer location is preserved. Such setup allows each of the nodes to take proactive measures even when the information exchange with other collaborating nodes is not possible. In the study presented herein, it is assumed that in addition to the information required for basic node positioning (i.e. inter-nodal range measurements, uncertainty, etc.), jammer coordinates estimated by each node can also be exchanged allowing for more accurate source localization.

The problem of determining jammers location by  $m$  nodes providing  $m$  node-jammer distance measurements can be formulated by defining a system of nonlinear equations that in its simplest form considered in this study would have two unknowns (for the 2-D cases) and  $m$  equations depending on the number of participating nodes. Such system of nonlinear equations is solved by the Least Squares method that requires an initial guess to start the execution. An issue with selecting initial guess far from correct solution is pointed in [12], which suggests that by doing so the optimization search could converge to local minima (as in correct case) leading to incorrect localization results.

In order to proceed with the localization of the RFI source within the cooperating network of users, the jamming signal first has to be detected. A number of different jamming detection techniques have been proposed both at precorrelation stage[13] and post-correlation stage[14]. As the focus of the study presented in this paper is on RFI source localization, detection is not considered further. For simplicity of implementation, prescient detection is assumed.

## 5. Experimental Setup

To evaluate the performance of the dynamic multi-node  $C/N_0$ -based RFI localization, a set of experiments have been conducted in a protected lab environment. For the study presented in this paper, two similar experiments were conducted in which the RFI source transmits omnidirectionally the wideband noise in the first experiment and a chirp jamming signal in the second. This section describes the scenario for the RFI localization along with the implementation details. The procedures to calibrate the receiver and interference simulation is also discussed later in this section.

### 5.1. Scenario Description

To simulate the operation of a collaborative navigation system, four identically equipped dynamic nodes were considered. Each of the nodes was moving along a predefined trajectory in a  $2\text{km} \times 2\text{km}$  region. For simplicity, it has been assumed that the nodes are operating in an area with good satellites visibility and no multipath or atmospheric effects. The simulated four nodes follow a rectilinear trajectory with varying dynamics, where each of the nodes (1,2,3 and 4) advances gradually in the operating environment with constant azimuths of  $135^\circ$ ,  $315^\circ$ ,  $225^\circ$ , and  $45^\circ$  respectively. Fig. 1 shows the velocity profile of individual nodes showing their behavior during the scenario.

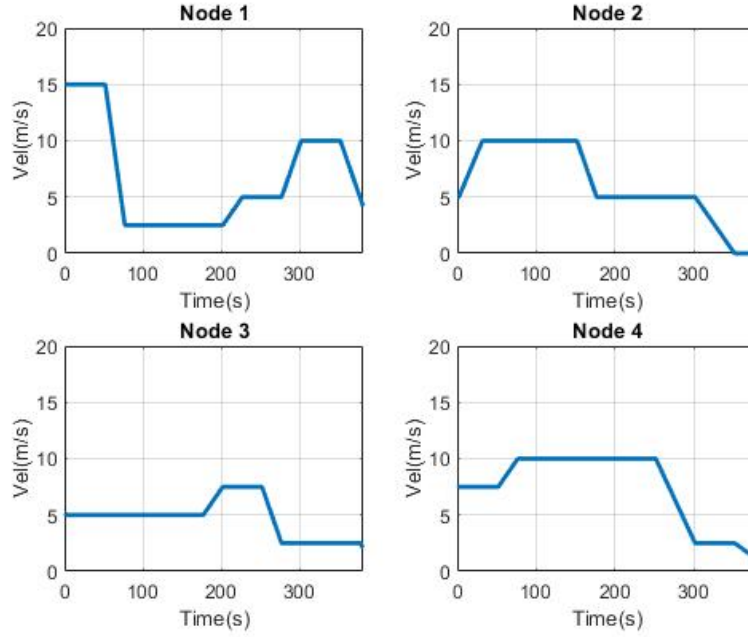


**Figure 1:** Nodes' kinematic profiles showing the magnitudes of the velocity vectors during the scenario. The x-axis shows the time values after the receivers give valid outputs.

## 5.2. Hardware Simulation Setup

The GNSS signals were generated by Spirent GSS8000 HW simulator and combined with an interfering signal generated by the Spirent MS3055 Interference Signal Generator. The combined signal was fed to the antenna input of the NovAtel OEM7 receiver. In the study presented herein, for implementation simplicity, only the GPS L1 C/A signal was considered. When running simulations, a number of received signal parameters including the  $C/N_0$  measurements were logged to a file by means of a command line utility provided by NovAtel. MATLAB was used for post-processing of the data.

The effects of wideband and chirp jamming on the average  $C/N_0$  values that are calculated using (4) are illustrated in Fig.2. The variations in the  $C/N_0$  values indicate the presence of a jamming source in the environment. They also highlight the time periods in the scenario, where the jammer is turned ON/OFF. As it can be observed from the plots in Fig.2, there is a slight difference between the level of degradation caused by the chirp jammer when compared to the wideband noise effect. This is due to the inherent characteristics of continuous frequency variations of the chirp signals. The maximum average  $C/N_0$  degradation is observed at the minimum distance of each node from the simulated jammer location. For the simulation scenario discussed in this paper, the jamming signal power levels have been selected high enough to cause substantial  $C/N_0$  degradation, but not complete loss of PVT capability.

## 5.3. RFI Emulation

To demonstrate the effect of RFI source and collect the data the algorithm, the jamming signal is injected for about 180 seconds during the scenario run. The duration of whole scenario is roughly 480 seconds (8 minutes), and the nodes follow the trajectories according to the assigned

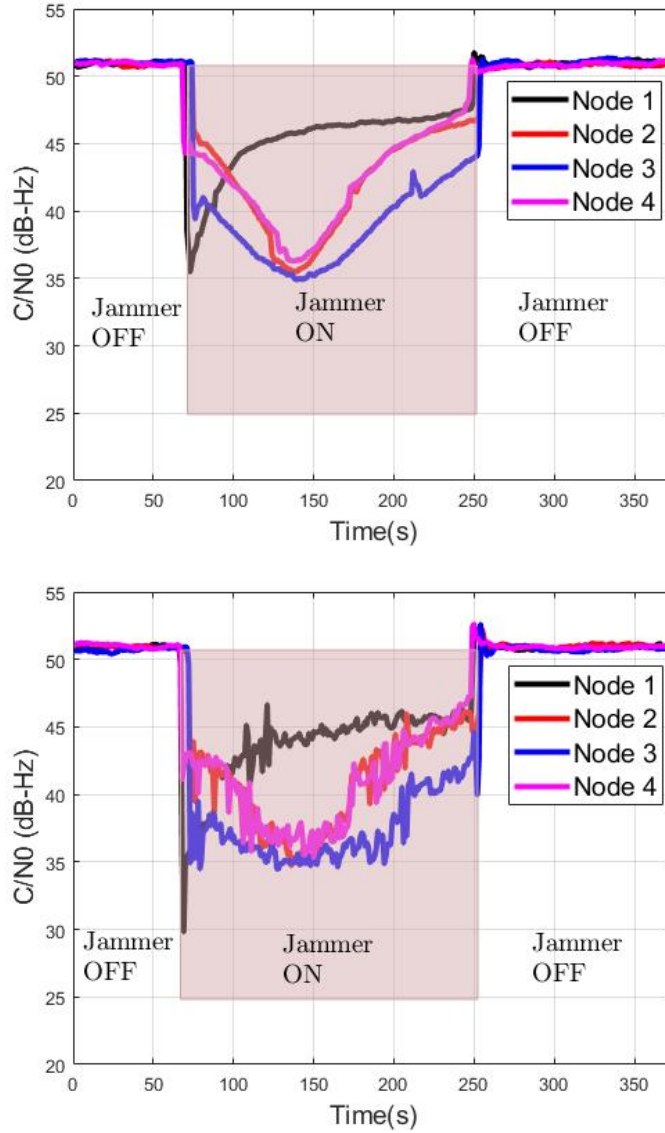


**Figure 2:** Average  $C/N_0$  Measurements in presence of Wideband (Top) and Chirp (Bottom) Jamming Signals

profiles. The jammer is turned ON at time  $t = 120$  sec and turned OFF at  $t = 300$  sec. In the simulation scenario presented in this paper, the power of the jammer is adjusted to avoid the loss of lock situations for most of the participating nodes. The jamming power of the wideband jamming signal is set to  $-55\text{dBm}$ . For the chirp case, the power level is set to  $-40\text{dBm}$ , while other design parameters are given in Table 1. It is reminded here that the frequency values are chosen to simulate an attack on GPS L1 signals only ( $f_{L1} = 1575.42$  MHz).

#### 5.4. Receiver Calibration

As stated earlier, in order to apply the synthetic phase array principle, it is necessary to calibrate the receiver performance in presence of jamming to determine the  $\bar{\beta}$  parameter. As

**Table 1**  
Chirp Jamming Signal Design Parameters

Signal Parameter	Value	Unit
$f_{start}$	1570.42	MHz
$f_{end}$	1580.42	MHz
No. of steps	50	-
Step Size	200	kHz
Dwell Time	10	ms
No. of pulses at each dwell	2000	-

discussed in [8], if not calibrated this parameter can impact the performance of the localization result, however, rough calibration is sufficient. The relationship of  $\bar{\beta}$  parameter with the average  $C/N_0$  output and the distance of a receiver from a reference location is given in (6). For the purpose of this study, it has been assumed that each of the cooperating nodes has the same set of navigation sensors, therefore, receiver calibration has been performed using only one GNSS receiver model, and the same beta value was applied for each of the nodes. The NovAtel OEM7 receiver used in this study was calibrated for wideband noise. The  $\bar{\beta}$ -factors are estimated to be 28 dB-Hz and also used in model given in (8).

## 6. Experimental Results

This section includes the discussion of the localization results both for the single user case discussed in Section 2 and multi-user case introduced in Section 4. Performance results of these approaches are quantified by calculating the Root Mean Square Error (RMSE) of the estimated jammer location. Results for Geometric Dilution of Precision (GDOP) are also presented to illustrate the impact of the node geometry on the solution.

### 6.1. Single User Scenario Results

To illustrate the results obtained in the single user/node case, solutions obtained for Nodes 1 and 3 will be used in this section. It is noted that as similar results were obtained for Nodes 2 and 4, they are not included in this paper to avoid repetition. An objective function of the form shown in (8) is defined using the averaged version of  $C/N_0$  measurements observed by each node,  $\beta$  value obtained after calibrating the receiver and the node's coordinates as measured during the simulation. Localization has been performed for different number of epochs  $N$  ( $N=2,10$  and  $20$ ) that in other words represents different lengths of the synthetic array. The samples are collected at the receiver's sampling rate 1 Hz, which means, for example,  $N = 2$  corresponds to 2 samples collected in 2 seconds. A solver based method is used to perform minimization without considering any constraints. The focus is on observing the results obtained by each of the nodes in a scenario attempting to localize the jammer independently. The jammer localization results for Nodes 1 and 3 in terms of the absolute error calculated as the difference between the known/simulated and estimated jammer position along East and North, as well as the obtained horizontal RMSE are shown in Tables 2 and 3.

As it can be observed from the results in Table 2, errors in the solution obtained by Node 1 are much larger compared to Node 3. This can be explained by Node 1 being further away from the jamming source during the simulation, and therefore much less affected. Due to



**Table 2**Node 1 Jammer Localization Results in Presence of Wideband Noise ( $\bar{\beta} = 28$  dB-Hz)

N	North[m]			East[m]			Horizontal[m]		
	Min	Max	RMSE	Min	Max	RMSE	Min	Max	RMSE
2	99.5	784.6	494.8	130.7	795.4	477	166.4	1108.9	687.3
10	127.3	782.6	466.3	167.4	820.6	514.2	210.3	985.4	694.1
20	162.7	509.7	205.5	205.5	643.1	503.7	262.1	820.6	654.3

**Table 3**Node 3 Jammer Localization Results in Presence of Wideband Noise ( $\bar{\beta} = 28$  dB-Hz)

N	North[m]			East[m]			Horizontal[m]		
	Min	Max	RMSE	Min	Max	RMSE	Min	Max	RMSE
2	1.9	551.7	223.5	0.5	640.5	226.2	3.1	794.4	317.9
10	11.8	562.3	229.4	6.6	293.8	182.1	14.8	634.4	292.8
20	1.1	271.2	170.2	7.7	265.6	168.8	7.8	379.6	239.7

**Table 4**Jammer Localization Results for Multi-User Scenario in Presence of Wideband Noise ( $\bar{\beta} = 28$  dB-Hz)

N	North[m]			East[m]			Horizontal[m]		
	Min	Max	RMSE	Min	Max	RMSE	Min	Max	RMSE
2	0.3	44.9	8.2	0.1	12.6	2.8	0.4	46.6	8.6
10	0.3	44.9	11.3	0.2	12.6	3.5	0.4	46.6	11.8
20	0.3	44.9	15.2	0.2	12.6	4.4	0.4	46.6	15.8

limited observability results obtained for Node 1 are much less accurate. While, the increase in estimation accuracy reflects the benefit of using more epochs to evaluate the cost function given in (8) using a longer period of time might not always be practical in dynamic scenarios.

## 6.2. Multi-User Scenario Results

This section discusses the results of collaborative localization when the nodes following the trajectories as illustrated in Section 5.1. Table 6 summarizes the results of the multi-user scenarios presenting the minimum, maximum and RMSE values for the horizontal position estimates. For fair comparison, same number of epochs have been considered as for single user scenario to get the estimates prior to combining the results. In comparison with the localization results of individual nodes discussed in previous subsection, considerable improvement in jammer location estimation is achieved, however, due to an increased RMSE considering the dynamic range, the less number of measurements does not seem to fit well in our model.

One of the factors impacting the accuracy of the estimated jammer location is the uncertainty in the position of the nodes. The difference between the simulated true and measured positions in terms of RMSE is shown in Fig.3. As mentioned earlier, good satellite visibility and no additional error sources have been simulated in this scenario. The only factors affecting the uncertainty in the position of the nodes are the node dynamics, receiver noise and the injected

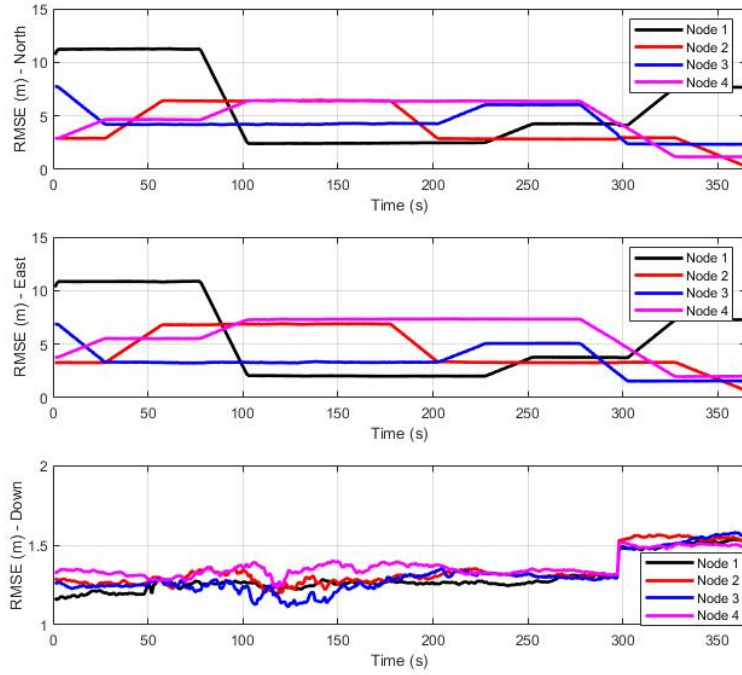


**Figure 3:** Root mean square error between true and observed NED components of nodes positions in presence of the wideband noise

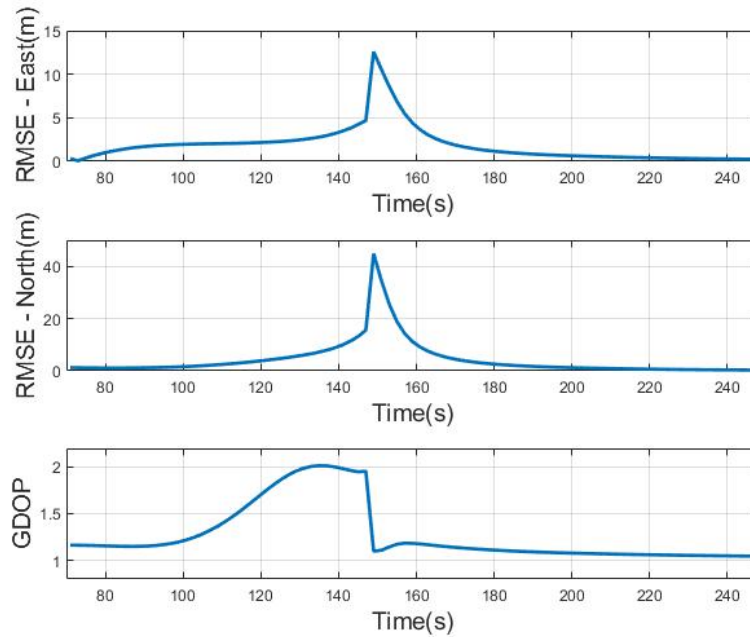
jamming signal.

Fig.4 shows the RMSE of the estimated jamming source location and GDOP result for the segment of the scenario when the jamming signal is injected considering the wideband noise jammer case. The error variance tends to increase when more measurements are included to localize the jammer.

It is also evident from the figure, node geometry has a significant impact on the result. The maximum RMSE of the jammer solution for wideband noise is at the instant when the nodes are not evenly distributed around the jammer clustering on one side in a nearly co-linear arrangement. The method to determine GDOP for various geometrical formations in 2-D cases is as described in [15]. Similar results were obtained for the chirp signal case, therefore they are not presented here to avoid repetition. Fig.5 illustrates best and worst case geometry examples for the simulated scenarios. As we can see in the case of the best GDOP, the nodes have good visibility volume of the jammer, which allows the nodes to accurately estimate the jammer location. In worst geometry case, the jammer is not even present inside the polygon formed by the nodes resulting in the maximum error in the jammer localization solution.

## 7. Conclusion

This paper extends the synthetic array based jammer localization concept [8] from a single user to a multi-user scenario. The basic principle behind this concept is based on a  $C/N_0$  model describing the impact of the received jamming power on the estimated  $C/N_0$  measurements.



**Figure 4:** Jammer Location RMSE (East, North) and GDOP for wideband noise jammer scenario ( $N=2$ ), the time shows the duration as the shaded region in Fig.2

Method discussion for a single user case implementation is provided and is extended for a multi-user scenario. To study the performance of this technique, a number of simulations performed in lab environments has been carried out considering a dynamic network of four nodes and a static jamming source. In a multi-node jamming localization case, it is observed that the localization accuracy depends on number of measurements considered to estimate the RFI source, and uncertainty of the node position and node-jammer geometry.

As indicated in [3], most of the jammers observed today are dynamic. Although only a simplified two dimensional case was considered in this paper, in a multi-node scenario where the jamming event is simultaneously observed by several nodes, more advanced results can be obtained including 3-D localization, and estimation of jamming source speed and direction of motion.

## References

- [1] Interface Control Document. ICD-GPS-200, Arinc Research Corporation, 11770 Warner Ave., Suite 210, Fountain Valley, CA, 1991.
- [2] J. Warburton, C. Tedeschi, GPS Privacy Jammers and RFI at Newark: Navigation Team AJP-652 Results, Technical Report I-GWG-12, 12th International GBAS Working Group Meeting,, Atlantic City, NJ, 2011.
- [3] M. Pattinson, M. Dumville, Y. Ying, D. Fryganiotis, M. Z. H. Bhuiyan, S. Thombre, H. Kuusniemi, A. Waern, P. Eliardsson, M. Pölöskey, S. Hill, V. Manikundalam, S. Lee, J. Gonzalez, Standardization of GNSS Threat Reporting and Receiver Testing through

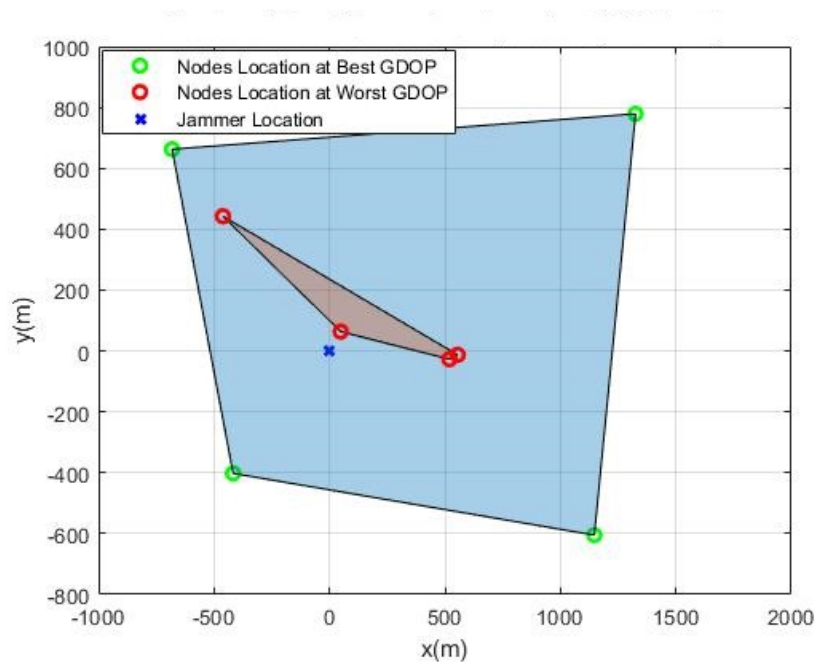


**Figure 5:** Best and Worst case node Geometry cases within the simulated scenario ( $N = 2$ )

- International Knowledge Exchange, Experimentation and Exploitation [STRIKE3] - Draft Standards for receiver testing, *European Journal of Navigation* 15 (2017) 4–8.
- [4] G. E. B. Berz, P. Barret, B. Disselkoen, M. Richard, V. Rocchia, F. Jacolot, T. Bigham, O. F. Bleker, Tracking RFI: Interference localization using a CRPA, *GPS World* (2017).
- [5] A. G. Dempster, E. Cetin, Interference Localization for Satellite Navigation Systems, *Proceedings of the IEEE* 104 (2016) 1318–1326.
- [6] J. Lindstrom, D. Akos, O. Isoz, M. Junered, GNSS Interference Detection and Localization using a Network of Low Cost Front-End Modules, in: *Proceedings of the 20th International Technical Meeting of the Satellite Division of The Institute of Navigation (ION GNSS 2007)*, Fort Worth, TX, 2007, pp. 1165–1172.
- [7] M. Trinkle, E. Cetin, R. Thompson, A. Dempster, Interference Localisation within the GNSS Environmental Monitoring System (gems) - Initial Field Test Results, in: *25th International Technical Meeting of the Satellite Division of the Institute of Navigation 2012, ION GNSS 2012*, volume 4, Nashville, TN, 2012, pp. 2930–2939.
- [8] D. Borio, C. Gioia, A. Štern, F. Dimc, G. Baldini, Jammer Localization: From Crowdsourcing to Synthetic Detection, in: *Proceedings of the 29th International Technical Meeting of the Satellite Division of The Institute of Navigation (ION GNSS+ 2016)*, Portland, Oregon, 2016, pp. 3107–3116.
- [9] J. Betz, Effect of Narrowband Interference on GPS Code Tracking Accuracy, *Proceedings of 2000 National Technical Meeting of the Institute of Navigation* (2000).
- [10] A. Kealy, G. Retscher, C. Toth, A. Hasnur-Rabiain, V. Gikas, D. Grejner-Brzezinska, C. Danezis, T. Moore, Collaborative Navigation as a Solution for PNT Applications in GNSS Challenged Environments – Report on Field Trials of a Joint FIG / IAG Working Group, *Journal of Applied Geodesy* 9 (2015).

- [11] A. Morrison, N. Sokolova, K. E. H. Eriksen, Collaborative navigation for defense objectives, in: 2015 International Conference on Indoor Positioning and Indoor Navigation (IPIN), Banff, AB, Canada, 2015, pp. 1–8.
- [12] D. Fontanella, R. Bauernfeind, B. Eissfeller, In-Car GNSS Jammer Localization with a Vehicular Ad-Hoc Network, in: Proceedings of the 25th International Technical Meeting of the Satellite Division of The Institute of Navigation (ION GNSS 2012), Nashville, TN, 2012, pp. 2885–2893.
- [13] A. Tani, R. Fantacci, Performance Evaluation of a Precorrelation Interference Detection Algorithm for the GNSS Based on Nonparametrical Spectral Estimation, *IEEE Systems Journal* 2 (2008).
- [14] D. Borio, C. Gioia, Real-time Jamming Detection using the Sum-of-Squares Paradigm, in: 2015 International Conference on Localization and GNSS (ICL-GNSS), Gothenburg, Sweden, 2015, pp. 1–6.
- [15] N. Levanon, Lowest GDOP in 2-D Scenarios, *IEE Proceedings - Radar, Sonar and Navigation* 147 (2000).